Methods 64 (2013) 305–314

Contents lists available at SciVerse ScienceDirect

Methods

journal homepage: www.elsevier.com/locate/ymeth

Label-free fluorescent DNA biosensors based on metallointercalators and nanomaterials

Shuo Shi [a,*], Xin Wang [b], Wenliang Sun [a], Xiangyang Wang [a], Tianming Yao [a,*], Liangnian Ji [a,c]

[a] Department of Chemistry, Tongji University, Shanghai 200092, PR China
[b] Shandong Institute for Prevention and Treatment of Endemic Disease, Jinan 250014, PR China
[c] MOE Laboratory of Bioinorganic and Synthetic Chemistry, School of Chemistry and Chemical Engineering, Sun Yat-Sen University, Guangzhou 510275, PR China

ARTICLE INFO

Article history:
Available online 15 July 2013

Keywords:
Biosensors
Metallointercalators
Nanomaterials
Label-free
Fluorescence

ABSTRACT

DNA based biosensors have become increasingly important in medical diagnostics, genetic and drug screening, and forensics in this post-genomic era. Chemical labeling methods suffer from several drawbacks, which are tedious, cost-expensive and time-consuming, thus the development of simple and general label free strategies is being demanded. The present article introduces a new model of biosensor device based on both metallointercalators and nanomaterials, with the aim of highlighting, in particular, the use of the "label-free" strategy for the construction of simple and inexpensive sensing platforms. In this work, two strategies were developed for designing "label-free" sensors: (1) metallointercalators act as the quencher to nanomaterials; (2) nanomaterials act as the quencher to metallointercalators. These methods take advantage of the sensitive luminescence signal change of metallointercalators or nanomaterials upon analytes binding. By monitoring the luminescence change, we were able to detect metal ions and biomolecules. Compared to other label-free fluorescent methods, these "label-free" DNA biosensors provide fast, simple, economical, sensitive and selective detection of target analytes with specific probes.

1. Introduction

Biosensors have become very popular in recent years. According to a recent IUPAC document [1], a biosensor is defined as an analytical device, which is capable of providing quantitative or semi-quantitative analytical information using a biological recognition element either integrated within or intimately associated with a physicochemical transducer. A biosensor comprises three parts [2–4]: (1) the sensitive elements (biologically derived material); (2) the transducer or detector element that transforms the detected signal into a readable, quantified output; and, (3) the signal processor that displays the transformed signal in a user-friendly way. In DNA biosensors the sensitive element is generally composed by single stranded DNA (ssDNA) molecules using the hybridization of complementary single-stranded molecules or a conformational transition of the aptamer DNA from an unfolded to a folded structure [5–8]. In recent years, the interest for DNA-based bisosensors has been growing. The development of the systems is motivated by applications in many fields: molecular diagnostics [9,10], pharmacogenomics [11,12], drug screening [13–15], medical diagnosis [16,17], food analysis [18–20], pesticide [21,22] and pollution [23,24] or environmental monitoring [25].

An ideal biosensor should achieve high sensitivity, high selectivity and maintain the rapidity and reusability of the devices. Many device designs have been investigated with the goal of creating simple, practical biosensor technologies. Optical methods are the most frequently used in the detection of analytes because of their simple and straightforward use [26,27]. One promising group of approaches is based on fluorescent signal evolution on optical transduction elements. Fluorescent DNA biosensors can be generally classified into two major types: label based and label free approaches. In recent years, a number of luminescent labeled detection methodologies have been developed, which are based on single-stranded oligonucleotides with the conjugation of a fluorophore at the end of the probe strand, or attachment of a fluorophore and a quencher at both ends of the probe DNA, whereby the presence of the targeted analyte would influence the spatial arrangement of fluorophore and quenchers in the labeled oligonucleotide or induce structure-switching of the labeled oligonucleotide. As summarized in many outstanding reviews, this kind of strategy has enjoyed consistent popularity due to its high target specificity, ease of operation, and the wide choice of fluorophores or quenchers available [28,29]. Though sensitive detection often results, such an approach needs to necessitate pre-labeling of the target sequence or the probe sequence, which is tedious, cost-expensive and time-consuming. Furthermore, labeling with various fluorescent and quenching molecules may affect the

* Corresponding authors.
E-mail addresses: shishuo@tongji.edu.cn (S. Shi), tmyao@tongji.edu.cn (T. Yao).

1046-2023/$ - see front matter © 2013 Elsevier Inc. All rights reserved.
http://dx.doi.org/10.1016/j.ymeth.2013.07.004

recognition event, potentially interfering with the sensitive and selective detection of the targeted analyte [30].

Therefore, label-free methods have attracted great interest because they are able to overcome these limitations as mentioned above. In the label-free approaches, fluorophores are not covalently attached to the nucleic acid backbone but instead interact noncovalently with DNA through a number of binding modes such as intercalation, groove-binding, end-stacking or electrostatic interactions. The luminescent molecules used in label-free DNA probes are generally non-emissive or only slightly emissive in aqueous solution resulting from quenching of the excited state by solvent interactions. However, they show enhanced luminescence upon binding to defined DNA structures due to the protection of their excited states within the hydrophobic interior of the oligonucleotide [30]. Consequently, the analyte-induced structure-switching of the functional oligonucleotide may be transduced into an optical output using a suitable luminescent molecule. One potential advantage of the label-free DNA-based approach is that the detection can be carried out in homogenous solution without any pre-labeling or immobilization step, greatly reducing the time and cost required for performing the assay.

Metallointercalators (including ruthenium, iridium and platinum complexes) have been widely employed for cellular imaging and molecular sensing [30–34]. These metallointercalators possess a variety of advantages, such as (i) high luminescence quantum yield, (ii) long phosphorescence lifetime that allows their emission to be distinguished from a fluorescent background, (iii) large Stokes shift for effective discrimination of excitation and emission wavelengths, (iv) sensitivity of their emissive properties to subtle changes in the local environment, and (v) modular synthesis that allows facile synthesis of analogs for fine-tuning of their chemical and/or photophysical properties [31–40]. The archetypical examples are the "molecular light switch" ruthenium(II) complexes $[Ru(L)_2(dppz)]^{2+}$ ((L) bpy (2,2′-bipyridine), phen (1,10-phenanthroline); dppz (dipyrido[3,2-a:2′,3′-c] phenazine)) developed by the Barton group in the early 1990s [41,42]. These complexes do not emit luminescence in aqueous solution upon photoexcitation of the metal-to-ligand charge transfer (MLCT) band, but emit luminescence brightly in the presence of duplex DNA [41–44]. This "light switch" effect is believed to arise from protection of the dppz nitrogens from water by intercalation in the base pairs of DNA; hydrogen-bonding and/or excited state proton transfer to these nitrogens by water quenches the emission [45]. It has also been reported that a minimum of six bases of the single stranded oligonucleotides are required for $[Ru(L)_2(dppz)]^{2+}$ to exhibit the light switch effect [46]. Our laboratory found that $[Ru(phen)_2(dppz)]^{2+}$ can serve as a prominent molecular "light switch" for both G-quadruplexes and i-motif, which prefers binding G-quadruplexes over i-motif [47,48]. Since then, many efforts have been made on the design and development of molecular "light switch" complexes based on the dppz ligand and its derivatives. Dunbar and Turro have achieved a chemical cycling of the molecular "light switch" on and off by successive additions of Co^{2+} ion and EDTA, respectively [49–52]. Our laboratory reported two new strategies for developing an on–off–on molecular "light switch" through the addition of $[Fe(CN)_6]^{2-}$ or utilizing pH value to control the "conformational switch" of G-quadruplex DNA [53,54]. These complexes have been used in a wide variety of applications, including DNA and protein detection, cell imaging, molecular-scale logic gates, and photoinduced electron-transfer reactions, among others [55–57].

More recently, our group has reported the application of metallointercalators as a highly selective luminescent probe for the detection of metal ions and biomolecules [58–61]. Herein, we describe the principles of the label-free fluorescent sensor based on metallointercalators (ruthenium complexes), with the aim of highlighting, in particular, the use of the "label-free" strategy for the construction of simple and inexpensive sensing platforms. The fluorescence of metallointercalators served as the signal to indicate the structure conversion of DNA. Compared to other label-free fluorescent methods, this approach provides easier operation and high sensitivity as well.

2. Principle of Methods

Simple, fast, sensitive, and cost-effective analysis of DNA is important in clinical diagnostics and treatment. Until now, several outstanding reviews of the applications of either nanomaterials or metallointercalators in DNA biosensors or DNA-based fabrication of nanomaterials were published [29–34,62–67]. There are mainly two purposes of using nanomaterials in DNA biosensors: as substrates for DNA attachment and as signal amplifiers for hybridization. On the other hand, metallointercalators that display a change in luminescent behavior upon binding DNA may be utilized as DNA structure indicator and signal generator. However, there are few researches focused on both nanomaterials and metallointercalator for DNA biosensors. In this context, we are aiming at introduce our proceeding works in recent years with a focus on the development of label-free DNA sensors by employing metallointercalators and nanomaterials. Two strategies developed by our group were introduced.

2.1. Metallointercalators act as the quencher to nanomaterials

Quantum dots are nanometer-sized luminescent semiconductor crystals that exhibit unique optical and electronic properties such as narrow, symmetric and stable fluorescence; and size-dependent, tunable absorption and emission [66–73]. Compared with conventional organic fluorescent dyes, the photoluminescence (PL) of quantum dots (QDs) possesses a variety of advantages, including high quantum yield, narrow, excellent photostability, and high photobleaching threshold. Thus, QDs have attracted considerable attention as novel luminescence indicators of different biological processes and bioanalysis in recent years [68–73].

Metal complexes have long been used as an effective quencher for luminescent organic and polymeric materials. Very recently, the interaction between CdSe and Ru complexes or Re complexes has been reported [74–76]. The mechanism of the luminescence of QDs affected by the metal complexes has always been the hot topic in different literatures. The possible mechanism could be the photoinduced electron transfer from the QDs to the Ru complex. In aqueous solution, water-soluble TGA-capped QDs carry the negatively charged carboxylate group. As a result, after the addition of Ru complex solution, the positively charged Ru complex and the negatively charged QDs form an ionic conjugate due to electrostatic attraction. Ru(II), which possesses partially filled d-orbitals and being the central ion of the Ru complex, is highly electrophilic and can work as a cationic electron acceptor. This static association between the Ru complex and QDs induces ultrafast photoinduced electron transfer from QDs to the electron acceptor, preventing the normal recombination of the electron and the hole in QDs, and results in a decrease of the fluorescent intensity of QDs [74–77].

Since the interaction of QDs with DNA molecules is weak and nonselective, direct detection of DNA through QD derivatives will not be a promising process. In this paper, we report a label free, sensitive and selective luminescence sensor for Ag(I) ions and thrombin using the molecular light switch $[Ru(bpy)_2(dppz)]^{2+}$ as both the quencher to quantum dots and a receptor to DNA (Scheme 1). After the addition of the Ru complex, the positively charged $[Ru(bpy)_2(dppz)]^{2+}$ and negatively charged water-soluble

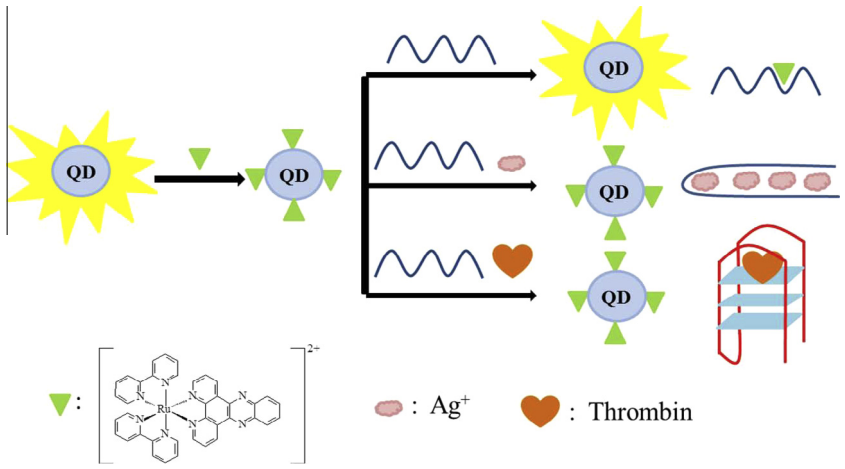

Scheme 1. Schematic description for label-free fluorescence detection of silver ions and thrombin based on molecular light switch Ru complex $[Ru(bpy)_2(dppz)]^{2+}$ and QDs.

TGA-capped CdTe quantum dots form an ionic conjugate due to their electrostatic attraction in aqueous solution. This static association results in a decrease of the fluorescent intensity of QDs. Upon addition of the C-rich (5′ CTC TCT CCA ACC TCT CTC 3′) single strand DNA (C-ssDNA), it could remove the quencher from the surface of QDs due to the strong DNA binding propensity of $[Ru(bpy)_2(dppz)]^{2+}$ [46], and the luminescence of QDs could be recovered. In the presence of Ag^+, C–Ag^+–C coordination induces the C-ssDNA to fold into a hairpin structure [78], which perturbs $[Ru(bpy)_2(dppz)]^{2+}$ to bind to C-ssDNA, resulting in significant quenching of the QDs fluorescence again. This sensing platform provides a simple, sensitive, and selective method for the detection of aqueous Ag^+. Similarly, when the thrombin-specific aptamer (5′-AGC CGT GGT AGG GCA GGT TGG GGT GACT-3′) was added, compared to the electrostatic association of the cationic ruthenium complex on the surface of QDs, it could remove the quencher from the surface of the nanoparticles due to the strong DNA binding affinity of the $[Ru(bpy)_2(dppz)]^{2+}$, resulting in the restoring the luminescence of the QDs at 560 nm [60]. When thrombin binds to the aptamer, the induced conformational change from random coil to quadruplex dissociates the ruthenium polypyridine complexes from the DNA. Thus, a decrease in the QDs emission was observed and could be used for the label-free detection of thrombin [58]. In addition, in aqueous solution, free $[Ru(bpy)_2(dppz)]^{2+}$ has no fluorescence, but it can produce red fluorescence at 610 nm after binding to DNA, whose luminescence intensity is much lower than that of QDs.

2.2. Nanomaterials act as the quencher to metallointercalators

Owing to their unique physical, chemical, and structural properties, graphene and its derivatives show outstanding potential in many fields, such as energy storage and conversion, high frequency electronics, and bioscience/biotechnologies [79–82]. Graphene oxide (GO), a two dimensional sheet resulting from acid exfoliation of graphite, offers a new class of solution-dispersible polyaromatic platforms for performing chemistry. Due to the presence of aromatic domains and functional groups, GO undergoes a complex interplay of ionic and nonionic interactions with different molecules in solution [79–83]. Graphene oxide is a good energy acceptor in energy transfer, it can act as a quencher to quench the fluorescence of organic dyes. What' more, GO can differentiate various DNA structures such as single-stranded DNA (ssDNA), double-stranded DNA (dsDNA) and stem-loops due to their characteristic interactions with GO. These interesting properties of GO have been exploited to develop a highly sensitive fluorescent DNA sensor [79–86]. The rationale is that GO interacts with dye-labeled DNA oligonucleotides and the proximity of the GO to the dye effectively quenches the fluorescence in the absence of a target. Conversely, in the presence of a target, the binding between dye labeled DNA and target molecule will alter the conformation of the dye-labeled DNA. The weak binding between dye-labeled DNA and the graphene surface means the dye is far away from the grapheme surface, resulting in restoration of dye fluorescence [81–84]. We herein report a label-free graphene-based strategy for DNA assay and aptamer-based potassium detection (Scheme 2). Compared to those methods mentioned above, it is easy, fast and inexpensive.

Ru polypyridine complexes have π-electron-rich framework. Here the Ru polypyridine complex $[Ru(bpy)_2(pip)]^{2+}$ (bpy = 2,2′-bipyridine; pip = 2-phenylimidazo[4,5-f] [1,10] phenanthroline) is taken for our assay. $[Ru(bpy)_2(pip)]^{2+}$ which has a strong binding affinity to DNA and can emit luminescence in Tris buffer at ambient temperature has been reported [87]. The positively charged Ru complex can interact with negatively charged GO to form a fluorescence-quenched charge-transfer complex, named hereafter Ru^+GO^-. When the Ru^+GO^- complex is reacted with DNA, the Ru^+GO^- complex can be broken because of a competitive binding of the Ru complex with DNA. Furthermore, the single-stranded DNA allows it to undergo π–π stacking on the GO surface, but does not remove the Ru complex from GO. However, when the DNA is double-stranded or can form G-quadruplex structure, Ru complex binding with DNA disturbs the interaction between the Ru complex and GO, resulting in the restoration of the Ru complex fluorescence. The efficient construction of the fluorescent sensor requires controllable proximity of the Ru complex to the graphene surface and obvious fluorescence changes. Thus, graphene oxide-Ru complex can be used as a platform for label-free fluorescence assay of a DNA sequence and potassium ions based on the exceptional quenching ability of GO towards the proximate Ru complex and the different propensities of ssDNA, dsDNA and G-quadruplex DNA to adsorb on GO.

3. Materials and methods

3.1. Materials and apparatus

$[Ru(bpy)_2(pip)]^{2+}$ and $[Ru(bpy)_2(dppz)]^{2+}$ were prepared and characterized according to the literatures [87,88]. All DNA synthesis reagents were ordered from Shanghai Sangon Biotechnology Co. Ltd. (Shanghai, China) and used without further purification. DNA

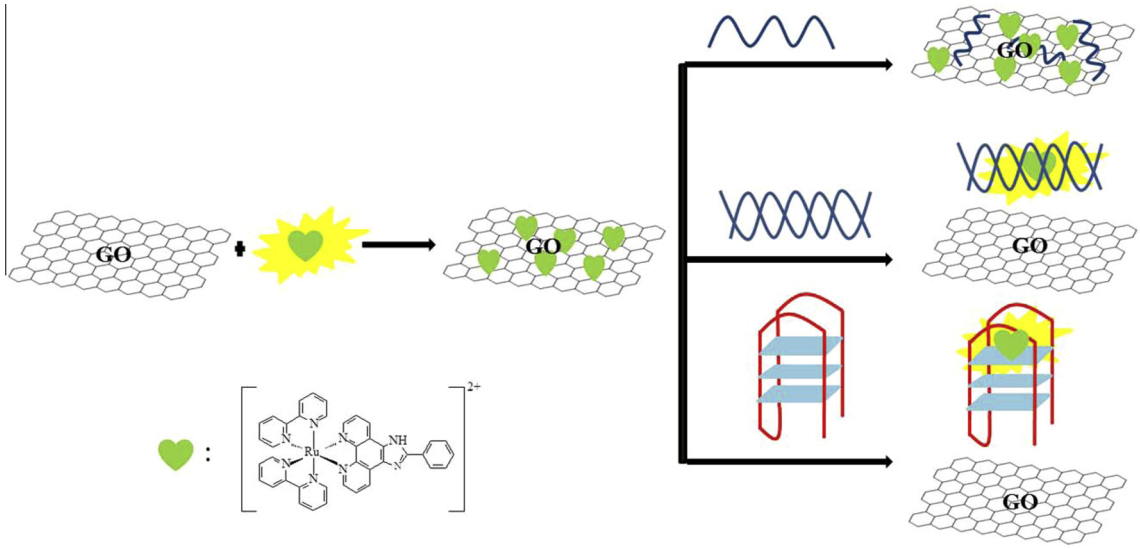

Scheme 2. Schematic description for detection of DNA and potassium ions based on the $Ru^{+}GO^{-}$/label-free DNA FRET.

stock solution was obtained by dissolving oligonucleotides in 10 mM Tris–HCl buffer (pH 7.4) and was stored at 4 °C before use. Concentrations of oligonucleotides were determined by measuring the absorbance at 260 nm after melting. Single-strand extinction coefficients were calculated from mononucleotide data using a nearest-neighbor approximation. Graphite powder of spectrographic grade was purchased from Sinopharm Chemical Reagent Co. Ltd. (China). All other reagents were of analytical grade.

Atomic force microscopy (AFM) was conducted with a Park AFM XE-100 microscope (Park Systems Corp.). Lambda Bio 40 UV/Vis Spectrophotometer (Perkin-Elmer, USA) was used to quantify the oligonucleotides and QDs. The PL spectra were recorded at room temperature on an F-7000 fluorescence spectrophotometer (Hitachi) with a quartz cell (2 mm). The excitation and emission slit width were both 10 nm. The FT-IR spectrum was recorded on a Nicolet 400 Fourier transform infrared spectrometer (Madison, WI).

3.2. Procedure for sample preparation

The synthesis of TGA (thioglycolic acid)-capped CdTe QDs was performed according to the reference with some modification [89]. First, NaHTe was prepared by adding 40 mg $NaBH_4$ to a flask containing 46 mg tellurium powder and 2 mL Milli-Q water under nitrogen atmosphere. The reaction was kept on for several hours until all tellurium powder was dissolved. 0.092 g (0.5 mmol) of $CdCl_2$ and 0.092 g (1 mmol) of thioglycolic acid were dissolved in 100 mL Milli-Q water, followed by adjusting pH to 8.2 by addition of 1 M NaOH solution. The mixture was deaerated by N_2 bubbling for 30 min. Then NaHTe solution (0.062 mmol) was quickly injected into the mixture under vigorous stirring, followed by refluxing the mixture for 2 h under open-air conditions. Both the size and concentration of the obtained QDs could be estimated from the UV–vis absorption spectrum.

The QD solution showed a photoluminescence peak at 560 nm. For the detection of quenching behavior of $[Ru(bpy)_2(dppz)]^{2+}$ on the fluorescence of QDs, 100 nM CdTe QDs and various amounts of $[Ru(bpy)_2(dppz)]^{2+}$ were incubated in 10 mM HEPES-NaOH buffer (pH 7.4) at room temperature for 5 min in a 0.5 mL Eppendorf tube respectively, then the fluorescence spectra were measured in 500 μL quartz cuvette at room temperature.

Graphene oxide (GO) was synthesized from natural graphite powder based on modified Hummers method [90,91]. Then, the as-prepared graphite oxide was subjected to ultrasonication for 30 min (1000 W, 20% amplitude). Finally, a homogeneous GO aqueous dispersion (1 mg mL^{-1}) was obtained and used for further use. $Ru^{+}GO^{-}$ complex was prepared as $[Ru(bpy)_2(pip)]^{2+}$ mixed with GO in 10 mM Tris–HCl buffer (pH 7.4). Resulting mixture was sonicated at 15–20 °C for 20 min to get $Ru^{+}GO^{-}$ complex (the final concentrations of $[Ru(bpy)_2(pip)]^{2+}$ and GO were 5 μM and 10 μg mL^{-1}, respectively).

3.3. Detection of target molecular

3.3.1. $[Ru(bpy)_2(dppz)]^{2+}$ as the quencher

For the fluorescence assay of metal ions: 10 μM C-ssDNA was incubated with different concentration of metal ions for 30 min, and then 10 μM $[Ru(bpy)_2(dppz)]^{2+}$ was added to allow it bind to DNA for 5 min. Next, 750 nM CdTe QDs were mixed with this solution and incubated at room temperature for 5 min. The resulting solutions were studied by fluorescent spectroscopy.

For the fluorescence assay of biomolecules: our strategy to detect thrombin was based on aptamers which are single-stranded DNA oligonucleotides that bind to their target molecules with high affinity. So a thrombin aptamer which is a 28-bases linear DNA (5′-AGC CGT GGT AGG GCA GGT TGG GGT GACT-3′) was chosen for detection. In a typical experiment, thrombin or other protein was added to 2.5 μM aptamer solution and the mixture was kept for about 30 min at room temperature. Then, Ru-QDs were added into this solution, and the mixture was incubated at room temperature for 5 min. The resulting solutions were studied by PL spectroscopy.

3.3.2. GO as the quencher

Fluorescence response of aptamer-$Ru^{+}GO^{-}$ towards metal ions: K^{+} aptamer 22AG (2.5 μM) was prepared in Tris–HCl buffer (10 mM, pH 7.4) and mixed with KCl for about 30 min at room temperature prior to the addition of $Ru^{+}GO^{-}$. The final K^{+} concentration in samples ranged from 50 μM to 500 μM. After allowing this mixture to bind, $Ru^{+}GO^{-}$ was added to reach equilibrium within 5 min, and then the fluorescence of the mixture was detected. The assay procedures for sodium, ammonium, lithium, copper, zinc, and magnesium ions (500 μM) were same as that for the potassium assay, except for using NaCl, NH_4Cl, LiCl, $CuCl_2$, $ZnCl_2$, and $MgCl_2$ instead of KCl.

To investigate dsDNA recognition, the 22AG (5′-A GGG TTA GGG TTA GGG TTA GGG-3′) was chosen for study. The target DNA sequence, T_1 (5′-C CCT AAC CCT AAC CCT AAC CCT-3′) and T_2 (5′-C AAT ATA AGA TTG AAA GGC GAT-3′), were 22 bases long and either perfectly complementary to the bases of 22AG or non-complementary strand, respectively. To recognize DNAs, $Ru^{+}GO^{-}$ was added to reach equilibrium within 5 min after 22AG mixed to T_1 or T_2 to hybridize for about 30 min, and then the fluorescence of the mixture was detected.

4. Results and discussion

4.1. Choice of metallointercalators

Metallointercalators have been attracted increasing attentions in DNA-associated studies, such as DNA foot-print, quantification, and DNA binding affinity study. This could be attributed to two major advantages of matallointercalator [92,93]: one is that the binding affinity of such complexes with DNA can be varied by easily altering the molecular structure of the ligands; the other is that the transition metal center offers a rich photo-physical [94] and electrochemical activity. Metallointercalators, being positively charged, are favored to bind to some negatively charged nanomaterials. As for the development of DNA sensors, metallointercalators and nanomaterials can act as an effective quencher each other. When metallointercalators act as the quencher to nanomaterials, the ideal metallointercalators should be non-emissive or only slightly emissive in aqueous solution resulting from quenching of the excited state by solvent interactions and could quench the luminescence of nanomaterials thoroughly at a low concentration. So $[Ru(bpy)_2(dppz)]^{2+}$ which was non-emissive in aqueous solution was selected in the first strategy. However, if nanomaterials act as the quencher of metallointercalators, the ideal metallointercalators should have strong luminescence either alone in aqueous solution or in the presence of DNA at a low concentration. In this case, luminescent metallointercalator $[Ru(bpy)_2(pip)]^{2+}$ was used instead of light switch complex $[Ru(bpy)_2(dppz)]^{2+}$.

4.2. Optimization of the measuring system

In order to obtain a highly sensitive response for the detection of target, the optimization of the conditions is essential. Buffer solution can not only affect the hybridization of DNA strands and DNA conformations, but also affect the fluorescence intensity of fluorophores [95,96]. For this reason, it is important to select an appropriate buffer for detection. Four kind buffers including PBS, HEPES, Tris–HCl and Tris-HAc were most frequently used. The pH value of the solution is another important factor affecting the performance of the sensor. A strong acidic environment will reduce the solubility of the DNA molecule and disturb its conformation, which eventually decreases the DNA hybridization and hence decreases the fluorescence intensity of fluorophores. On the other hand, some cations and nanomaterials will precipitate in an alkaline condition. Therefore, detections of analyte were often performed within a narrow pH range from 6.0 to 8.0. Commonly, pH 7.4, a mild condition, was used in this study.

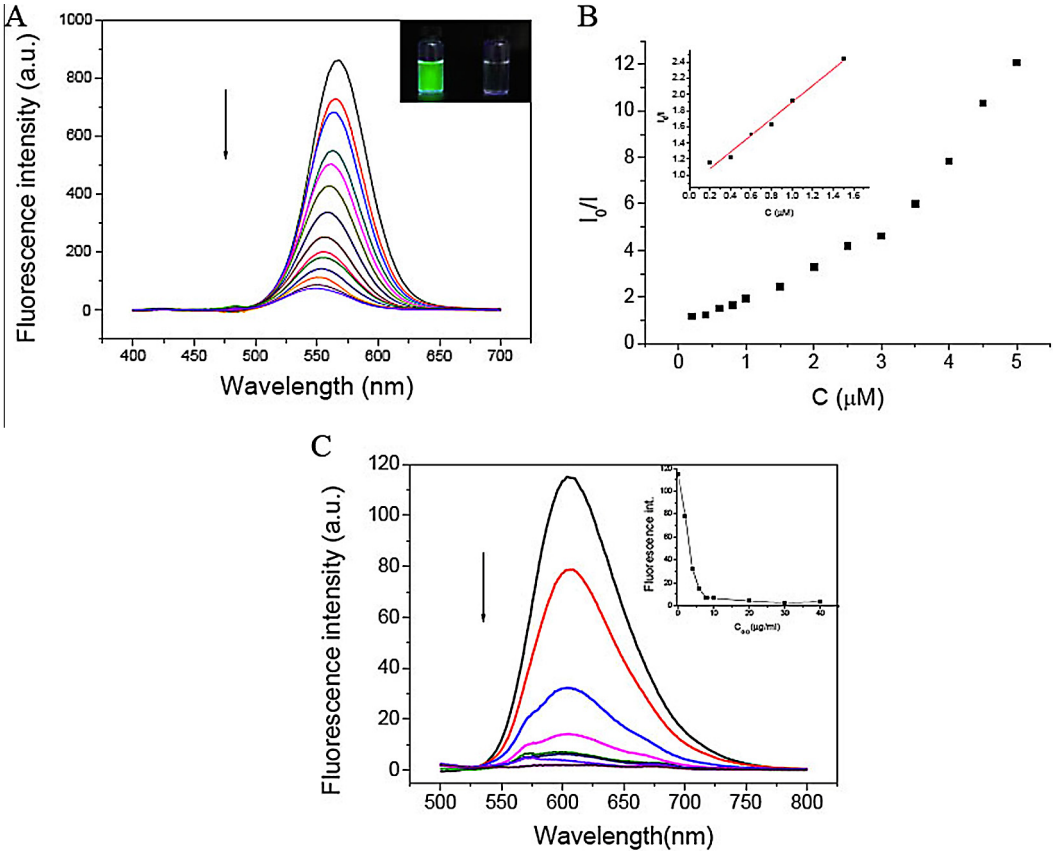

Fig. 1. (A) Changes in the fluorescence spectra of TGA-capped CdTe QDs (100 nM) in 10 mM Tris–HCl (pH 7.4), with increasing concentration of $[Ru(bpy)_2(dppz)]^{2+}$, with concentrations of 0, 0.2, 0.4, 0.6, 0.8, 1.0, 1.5, 2.0, 2.5, 3, 3.5, 4, 4.5, 5 M (from top to bottom). Inset: fluorescence image of CdTe QDs (100 nM) in the absence (left) and presence (right) of 5 M $[Ru(bpy)_2(dppz)]^{2+}$. (B) Stern–Volmer plot of QD quenched by $[Ru(bpy)_2(dppz)]^{2+}$ in buffer solution. Excitation: 365 nm, emission: 560 nm. (C) Fluorescence spectra of $[Ru(bpy)_2(pip)]^{2+}$ complex (5 μM) with different amounts of GO ranging from 0 to 40 μg mL^{-1}. Inset: fluorescence intensity of $[Ru(bpy)_2(pip)]^{2+}$ and GO plotted against the concentration of GO. Excitation: 455 nm, emission: 605 nm. Data are adopted from a previous study [58–60].

In order to establish a fluorescence-quenched system, the concentrations of nanomaterials and metallointercalators are key factors. Given the fluorescence intensity and solubility of nanomaterials and metallointercalators, an appropriate concentration is necessary. To investigate the quenching behavior of $[Ru(bpy)_2(dppz)]^{2+}$ on the fluorescence of CdTe QDs, the fluorescence signals toward different concentrations of Ru complex were measured in 10 mM HEPES-NaOH buffer (pH 7.4). As shown in Fig. 1A, The QDs solution showed a photoluminescence peak at 560 nm. The fluorescence quenching ability of $[Ru(bpy)_2(dppz)]^{2+}$ was evaluated via fluorescence measurements of 100 nM QDs in the presence of $[Ru(bpy)_2(dppz)]^{2+}$. With the increasing concentration of Ru complex, the fluorescence intensity of QDs decreased and trended to a minimum value at 5 μM. Thus, 5 μM $[Ru(bpy)_2(dppz)]^{2+}$ was used for analytical purpose, and it can interact with QDs (100 nM) to form a fluorescence-quenched complex, named hereafter Ru-QDs. From the dependence of fluorescence intensity of QDs on $[Ru(bpy)_2(dppz)]^{2+}$ concentration, the fluorescence

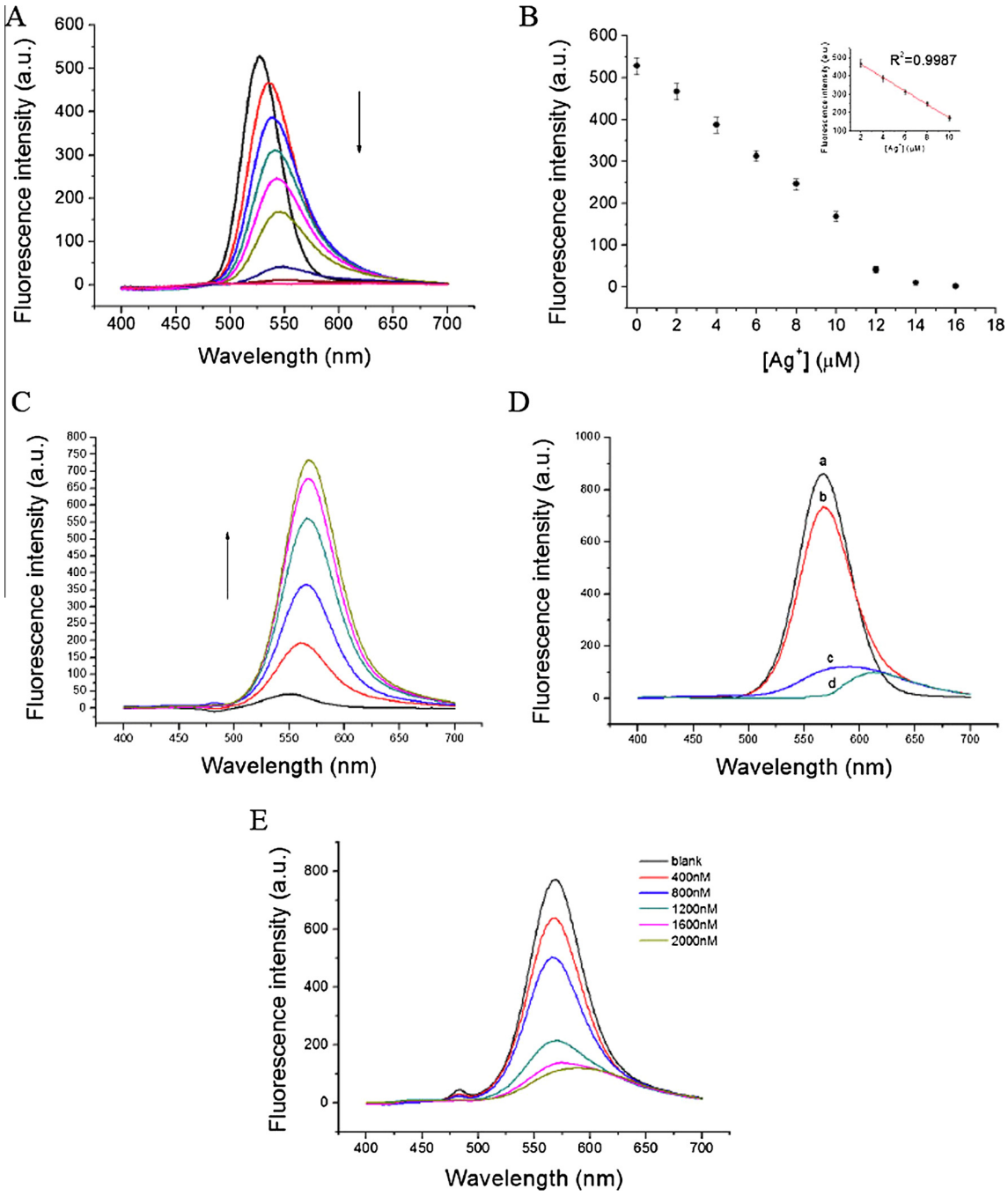

Fig. 2. (A) Fluorescence spectra of the QDs–Ru complex with 10 μM DNA in the presence of different concentrations of Ag^+ (from top to bottom: 0, 2, 4, 6, 8, 10, 12, 14, and 16 μM); (B) plots of the fluorescence intensity against the concentration of Ag^+. Inset: linear relationship between fluorescence intensity and Ag^+ concentrations (2–10 μM); (C) fluorescent spectra of 100 nM TGA-capped CdTe and 5 μM $Ru(bpy)_2dppz^{2+}$ in the presence of aptamer with concentrations of 0, 0.5, 1, 1.5, 2, and 2.5 μM (from bottom to top); (D) fluorescence emission spectra at different conditions: (a) 100 nM QDs in Tris–HCl buffer; (b) 100 nM QDs + 5 μM $Ru(bpy)_2(dppz)^{2+}$ + 2.5 μM DNA; (c) 100 nM QDs + 5 μM $Ru(bpy)_2(dppz)^{2+}$ + 2.5 μM DNA + 2000 nM Thrombin; (d) 5 μM $Ru(bpy)_2(dppz)^{2+}$ + 2.5 μM DNA; (E) fluorescence emission spectra of Ru–QDs and aptamer in the presence of different concentrations of thrombin. Black curve is the fluorescence emission of control probes (same volume of buffer added) without target. Excitation: 365 nm. Data are adopted from a previous study [58,59].

quenching could be described by the Stern–Volmer equation with a quenching constant of 9.62×10^5 M, and the linear range is from 2×10^{-7} M to 1.6×10^{-6} M (Fig 1B). Similarly, the fluorescence intensity of $[Ru(bpy)_2(pip)]^{2+}$ decreased with increased concentration of graphene oxide (Fig. 1C). It can be seen that the fluorescence of the Ru complex (5 μM) is quenched almost completely by GO (10 μg mL^{-1}) and the quenching efficiency is estimated to be 98%. In our report, without special mentioned, the final concentrations of $[Ru(bpy)_2(pip)]^{2+}$ and GO were 5 μM and 10 μg mL^{-1}, respectively.

Besides these factors, ionic strength, incubation temperature and reaction time affect the sensitivity and selectivity under certain conditions.

4.3. Sensitivity

To investigate our strategy for the detection of analyte, different experiments were carried out. For example, the emission of DNA/QDs-Ru as a function of Ag^+ concentration was measured. The effect of different concentrations of Ag^+ on the fluorescence spectra of the DNA/QDs-Ru system is shown in Fig. 2A. As the concentration of Ag^+ increased, the fluorescence intensity decreased. Furthermore, upon addition of Ag^+ makes the fluorescence emission peak shift slightly to longer wavelength. The reason may be that the binding of Ag^+ changes the electronic properties of the base pairs and Ru complex, and the electron transfer between donor and receptor, leading to the observed red-shift. From the results shown in Fig. 2B, a linear relationship ($R^2 = 0.9987$) of the Ag^+ concentration with the fluorescence emission intensity was observed in the concentration range of 2–10 μM. We estimated that the limit of detection (LOD) for Ag^+ ions, at a signal-to-noise of 3, was 0.1 μM.

Based on this principle, thrombin was detected too. In a typical experiment, thrombin was added to 2.5 μM aptamer solution and the mixture was kept for about 30 min at room temperature. With the increasing concentration of aptamer added into Ru-QDs, the fluorescence emission intensity of QDs increased. After adding 2.5 μM aptamer, the fluorescence intensity of QDs almost restored (Fig. 2C). However, in the presence of thrombin, the fluorescence of QDs was quenched by the Ru complex again due to the formation of quadruplex–thrombin complexes (curve c, Fig. 2D). It is reasonable that aptamers bind preferentially to thrombins because of the high affinity between aptamers and thrombin. It should be noted that a fluorescent output at 610 nm was observed induced by DNA binding of Ru complex (curve d, Fig. 2D). However, the fluorescence intensity is much lower than that of QDs. So, the fluorescence output of the QDs at 560 nm was utilized in our assay. Fig. 2E shows the fluorescence intensity of Ru-QDs and aptamer at various concentrations of thrombin. The fluorescence intensity decreased when thrombin was added into the aptamer. Over 80% fluorescence was quenched by Ru complex when aptamer incubated with 1600 nM thrombin. A detection limit down to 50 nM at a signal-to noise ratio (S/N) of 3:1 was achieved.

Graphene oxide–Ru complex can be used as a platform for label-free fluorescence assay of a DNA sequence and potassium ions based on the exceptional quenching ability of GO towards

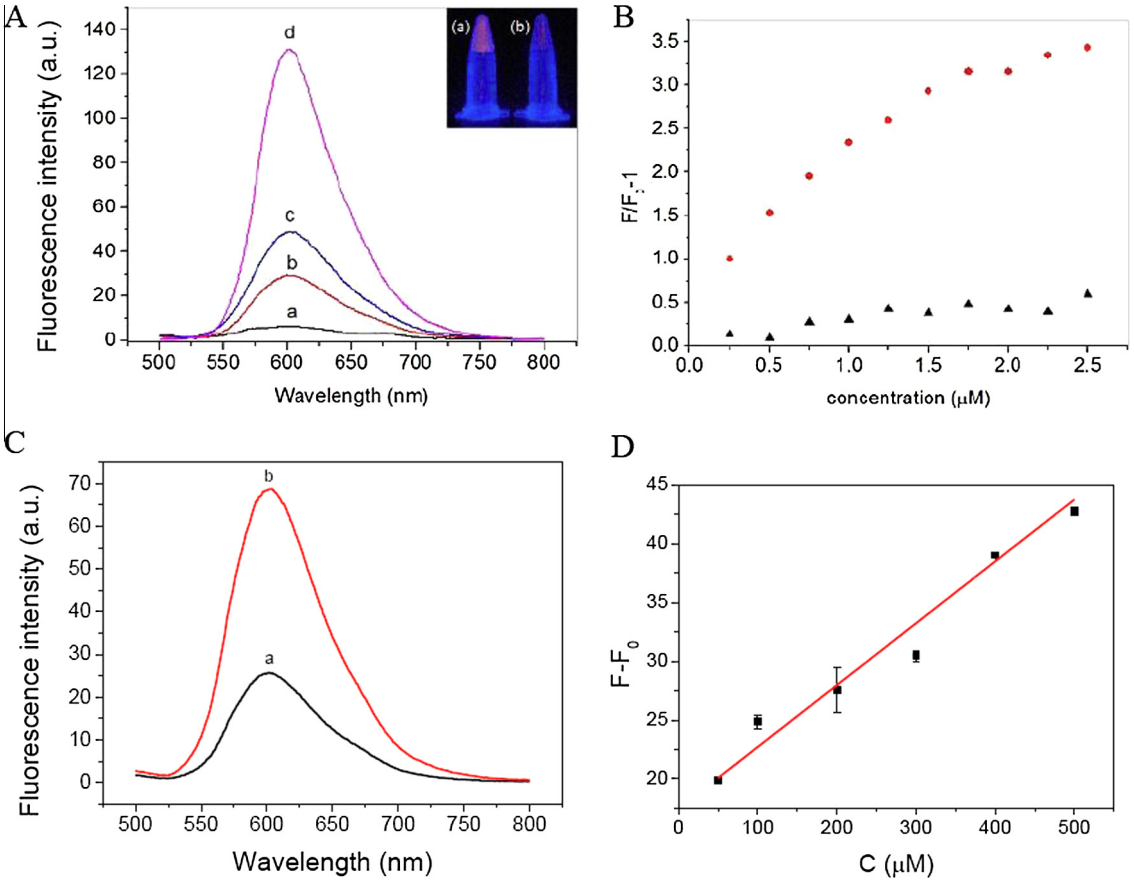

Fig. 3. (A) Fluorescence emission spectra (excitation at 455 nm) of Ru^+GO^- at different conditions: (a) Ru^+GO^- in Tris–HCl buffer; (b) Ru^+GO^- + 22AG (2.5 μM); (c) Ru^+GO^- + 22AG (2.5 μM) + T_2 (2.5 μM); and (d) Ru^+GO^- + 22AG (2.5 μM) + T_1 (2.5 μM). Inset: fluorescence image of Ru^+GO^- (Ru complex: 40 μM, GO: 80 μg ml^{-1}) with (a) 22AG (83.3 μM) + T_1 (83.3 μM); (b) 22AG (83.3 μM) + T_2 (83.3 μM). All the photos were taken under a 365 nm UV lamp; (B) fluorescence intensity ratio of complementary DNA (●) and non-complementary DNA (▲) with (F/F_0−1) plotted against the concentration of DNA; (C) fluorescence emission spectra of Ru^+GO^- with 2.5 μM 22AG incubated in (a) Tris–HCl buffer without K^+; (b) Tris–HCl buffer containing 500 μM KCl. (D) Fluorescence intensity changes of Ru^+GO^- with $F-F_0$ plotted against K^+ concentration. Excitation: 455 nm, emission: 605 nm. Data are adopted from a previous study [60].

the proximate Ru complex and the different propensities of ssDNA, dsDNA and G-quadruplex DNA to adsorb on GO. It can be seen that the fluorescence of the Ru complex is quenched almost completely by GO (Fig. 3A, curve a). Addition of 22AG to $Ru^{+}GO^{-}$ solution caused fluorescence enhancement through ssDNA binding (Fig. 3A, curve b). Meanwhile, the $Ru^{+}GO^{-}$ had significant fluorescence enhancement upon addition of dsDNA formed by 22AG and T_1 in 10 mM Tris–HCl buffer (pH 7.4) (Fig. 3A, curve d). $Ru^{+}GO^{-}$/22AG exhibited a significant difference in the response to T_2 and T_1 (Fig. 3A, curve c). Inset to Fig. 1A reveals that in comparison to ssDNA, the fluorescence enhancement of $Ru^{+}GO^{-}$ towards dsDNA was apparent. In the case of non-complementary DNA T_2, no obvious significant variation in the fluorescence intensity was found. However, for the complementary DNA T_1, a dramatic increase in the fluorescence intensity was observed (Fig. 3B). By the way, in the absence of GO, the fluorescence intensity differences of Ru complex between ssDNA and dsDNA were not obvious [60]. Meanwhile, we used the similar strategy to detecte K^{+}. The K^{+} aptamer is a G-rich ssDNA (22AG) and is random-coil like in solution without K^{+}. Upon binding to its target (K^{+}), the aptamer folds into a four-stranded G-quadruplex structure via intramolecular hydrogen bonds between guanines [95,96]. In our experiment, we compared the emission spectra observed upon addition of $Ru^{+}GO^{-}$ to solutions of 22AG in the absence or presence of 500 μM KCl. The DNA resumes a G-quadruplex and random coil structures in the presence and absence of KCl, respectively. This was illustrated by the fluorescence, which increased approximately two-fold upon 22AG in the presence of 500 μM K^{+} (Fig. 3C). The fluorescence intensity changes ($F–F_0$) of the sensor was examined with 22AG incubation in different concentrations of K^{+} in 10 mM Tris–HCl (pH 7.4), where F, F_0 are the fluorescence intensity of $Ru^{+}GO^{-}$ with 22AG incubation in the presence and absence of K^{+}, respectively (Fig. 3D). Significantly, fluorescence intensity change was obvious at as low as 100 μM of K^{+}, suggesting that $Ru^{+}GO^{-}$ was sensitive probe for aptamer structure. We also tested the power of the detection for K^{+} using Ru complex alone. In the absence of GO, Ru complex hardly discriminates G-quadruplex from random coil structure by Ru complex fluorescence enhancement [60].

4.4. Selectivity

The selectivity of Ru-QDs based detection system for Ag^{+} was investigated. Fig. 4A shows the value of F/F_0-1 between the blank and solutions containing Ag^{+} (15 μM) or other metal ions (Li^{+}, Na^{+}, K^{+}, Cu^{2+}, Co^{2+}, Ni^{2+}, Mg^{2+}, Ca^{2+}, Cd^{2+}, Zn^{2+}, Pb^{2+}) (50 μM), where F_0 and F are the fluorescence intensity of DNA/QDs-Ru without and with metal ions, respectively. The selectivity of this Ru-QDs based detection system for thrombin was also investigated. As indicated in Fig. 3C, control experiments were performed using bovine serum albumin (BSA) and lysozyme. It was revealed that these proteins had little effect on the separation of Ru complex from aptamer, showing that the platform was specific to thrombin response.

The selectivity of $Ru^{+}GO^{-}$ detection system for K^{+} was investigated too. Aptamers have high binding specificity, we examined the effect of a variety of monovalent and divalent cations (Li^{+}, Na^{+}, K^{+}, NH_4^{+}, Mg^{2+}, Cu^{2+}, Zn^{2+}) at 500 μM. High selectivity for K^{+} over Li^{+}, Na^{+}, K^{+}, NH_4^{+}, Mg^{2+}, Cu^{2+}, Zn^{2+} was observed, thus this $Ru^{+}GO^{-}$/aptamer could be used as a sensitive and selective platform for K^{+} detection. Therefore the principle described in this work can be conveniently generalized to other aptamer systems.

By using C-rich oligonucleotide for specific C–Ag^{+}–C interaction, we demonstrate the successful use of QDs and molecular light

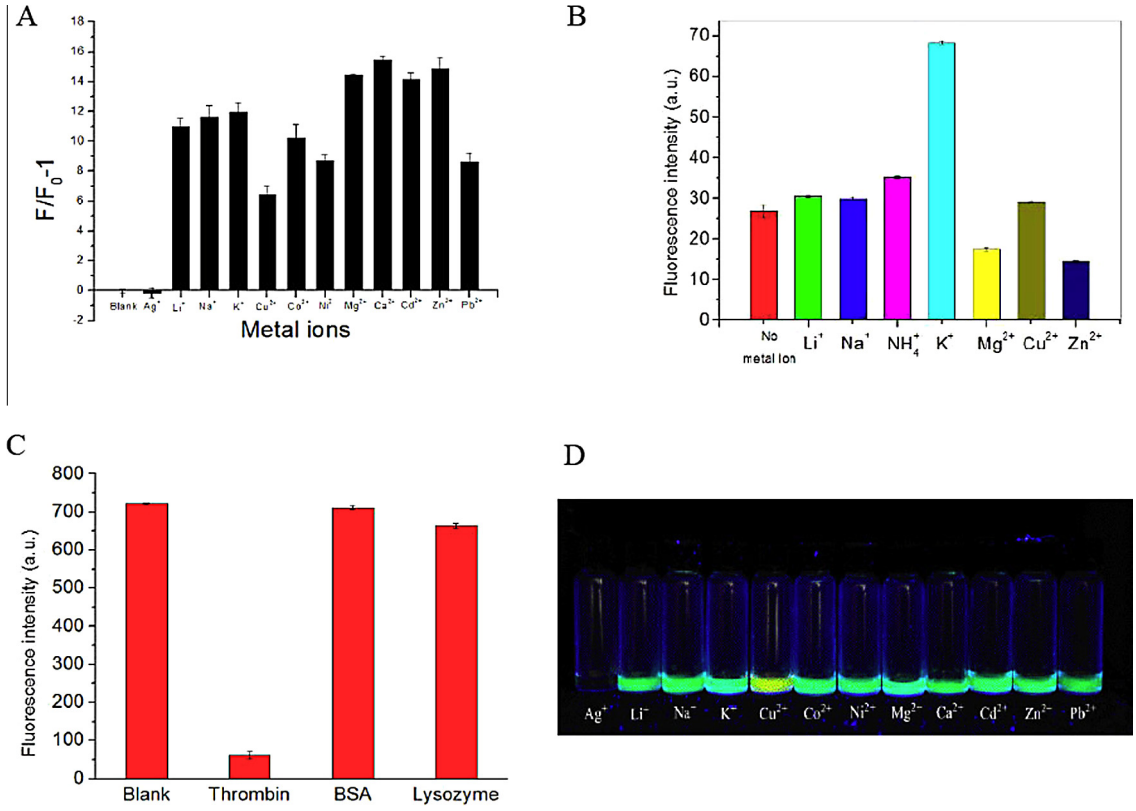

Fig. 4. (A) Selectivity of the sensor to different metal ions. The fluorescence intensities were recorded at 530 nm. Excitation: 365 nm; (B) the fluorescence intensity of $Ru^{+}GO^{-}$ adding 22AG (2.5 μM) incubation with various metal ions (metal ion: 500 μM). Excitation: 455 nm, emission: 605 nm; (C) the PL signals of biosensor response to 2 μM thrombin, BSA and lysozyme. Excitation: 365 nm, emission: 560 nm; (D) photographs of the sensor in the presence of various metal ions under a 365 nm UV lamp. The concentration of Ag^{+} is 15 μM; concentrations of the other metal ions are 50 μM. All measurements were done in 10 mM HEPES-NaOH buffer. Data are adopted from a previous study [58–60].

switch Ru complex as an effective, label-free fluorescent sensing platform for Ag^+ detection. Furthermore, this detection selectivity could be visualized with the naked eye (Fig. 4D).

5. Conclusions and future prospects

Metallointercalators have been attracted increasing attentions in DNA-associated studies, such as DNA foot-print, quantification, and DNA binding affinity study. Due to the high DNA binding affinity of such metallointercalators, metallointercalators alone as a DNA probe are limited by the relatively modest selectivity for duplex DNA over other conformations such as single-stranded DNA or G-quadruplex, thereby somewhat negating the potent advantages of sensitivity and selectivity offered by nucleic acid aptamers or other functional oligonucleotides. To overcome this limitation, we propose a label-free DNA based biosensor for the selective detection of analyte using both metallointercalators and nanomaterials. Either nanomaterials or metallointercalators play an essential role of signal generator or signal quencher. Utilizing these strategies, we have successfully realized the detection of cations and biomoleculars, even with naked eye. These sensors possess several superiorities over the previous optical sensors, which is label-free, simple, and cost-effective. With the development of label free DNA based biosensors, it can be anticipated that, in a near future, the advanced biosensors may all exhibit high sensitivity, good stability and satisfactory selectivity for the detection of many important disease-associated molecules, which may be of great clinical significance in the diagnosis and treatment of diseases.

Acknowledgments

This work was supported by the National Natural Science Foundation of China (20901060, 31170776, 81171646) and the Fundamental Research Funds for the Central Universities.

References

[1] D.R. Thevenot, K. Toth, R.A. Durst, G.S. Wilson, Pure Appl. Chem. 7 (1999) 2333–2348.
[2] C.F. Ding, H. Li, K.C. Hu, J.M. Lin, Talanta 80 (2010) 1385–1391.
[3] C.F. Ding, Y. Ge, J.M. Lin, Biosens. Bioelectron. 25 (2010) 1290–1294.
[4] A. Liu, K. Wang, S.H. Weng, Y. Lei, L.Q. Lin, W. Chen, X.H. Lin, Y.Z. Chen, Trends Anal. Chem. 37 (2012) 101–111.
[5] M. Campàs, I. Katakis, Trends Anal. Chem. 23 (2004) 49–62.
[6] R.J. Hamers, Nature 454 (2008) 708–709.
[7] A.P.F. Turner, Chem. Soc. Rev. 42 (2013) 3184–3196.
[8] S. Cagnin, M. Caraballo, C. Guiducci, P. Martini, M. Ross, M. SantaAna, D. Danley, T. West, G. Lanfranchi, Sensors 9 (2009) 3122–3148.
[9] R.E. Wang, Y. Zhang, J. Cai, W. Cai, T. Gao, Curr. Med. Chem. 18 (2011) 4175–4184.
[10] X. Mao, Y. Ma, A. Zhang, L. Zhang, L. Zeng, G. Liu, Anal. Chem. 81 (2009) 1660–1668.
[11] S.E. Tolley, H.K. Wang, R.S. Smith, D.A. Christensen, J.N. Herron, Anal. Biochem. 315 (2003) 223–237.
[12] R. Sosnowski, M.J. Heller, E. Tu, A.H. Forster, R. Radtkey, Psychiatry Genet. 12 (2002) 181–192.
[13] M. Minunni, S. Tombelli, M. Mascini, A. Bilia, M.C. Bergonzi, F.F. Vincieri, Talanta 65 (2005) 578–585.
[14] J.F. Rusling, E.G. Hvastkovs, D.O. Hull, J.B. Schenkman, Chem. Commun. 2 (2008) 141–154.
[15] H. Wang, T. Chen, S. Wu, X. Chu, R. Yu, Biosens. Bioelectron. 34 (2012) 88–93.
[16] G.P. Nikoleli, D.P. Nikolelis, N. Tzamtzis, Intelligent Nanomater. (2012) 783–800.
[17] H. Shi, T. Xia, A.E. Nel, J.I. Yeh, Nano. Med. 2 (2007) 599–614.
[18] C. Calas-Blanchard, M. Cortina-Puig, L. Barthelmebs, T. Noguer, Curr. Anal. Chem. 8 (2012) 428–435.
[19] P. Kara, O. Kilickaya, Control (2011) 123–134.
[20] H. Sharma, R. Mutharasan, Sen. Actuat. B 183 (2013) 535–549.
[21] A. Sassolas, B. Prieto-Simón, J.L. Marty, Am. J. Anal. Chem. 3 (2012) 210–232.
[22] T.F. Kang, Y. Xiong, R. Xue, S.Y. Cheng, Anal. Lett. 46 (2013) 1255–1266.
[23] L. Wu, X. Lu, J. Jin, H. Zhang, J. Chen, Biosens. Bioelectron. 26 (2011) 4040–4045.
[24] P. Venier, C. DePitta, A. Pallavicini, F. Marsano, L. Varotto, C. Romualdi, F. Dondero, A. Viarengo, G. Lanfranchi, Mutat. Res. 602 (2006) 121–134.
[25] M.J. LaGier, J.W. Fell, K.D. Goodwin, Mar. Pollut. Bull. 54 (2007) 757–770.
[26] M. Schaferling, S. Nagl, Anal. Bioanal. Chem. 385 (2006) 500–517.
[27] A. Sassolas, B.D. Leca-Bouvier, L.J. Blum, Chem. Rev. 108 (2008) 109–139.
[28] X.B. Zhang, R.M. Kong, Y. Lu, Annu. Rev. Anal. Chem. 4 (2011) 105–128.
[29] Y. Du, B. Li, E. Wang, Acc. Chem. Res. 46 (2013) 203–213.
[30] D.L. Ma, H.Z. He, K.H. Leung, H.J. Zhong, D.S.H. Chan, C.H. Leung, Chem. Soc. Rev. 42 (2013) 3427–3440.
[31] Q. Zhao, F. Li, C. Huang, Chem. Soc. Rev. 39 (2010) 3007–3030.
[32] D.L. Ma, V.P.Y. Ma, D.S.H. Chan, K.H. Leung, H.Z. He, C.H. Leung, Coord. Chem. Rev. 256 (2012) 3087–3113.
[33] D.L. Ma, D.S.H. Chan, H. Yang, H.Z. He, C.H. Leung, Curr. Pharm. Design 18 (2012) 2058–2075.
[34] M.Y. Wei, L.H. Guo, P. Famouri, Microchim. Acta 172 (2011) 247–260.
[35] S. Shi, H. Huang, X. Gao, J. Yao, C. Lv, J. Zhao, W. Sun, T. Yao, L. Ji, J. Inorg. Biochem. 121 (2013) 19–27.
[36] J. Yao, X. Gao, W. Sun, S. Shi, T. Yao, Dalton Trans. 42 (2013) 5661–5672.
[37] S. Shi, C. Lv, X. Gao, J. Zhao, J. Yao, W. Sun, H. Huang, T. Yao, L. Ji, Inorg. Chem. Commun. 24 (2012) 212–215.
[38] K.H. Leung, H.Z. He, V.P.Y. Ma, D.S.H. Chan, C.H. Leung, D.L. Ma, Chem. Commun. 49 (2013) 771–773.
[39] C.H. Leung, D.S.H. Chan, H.Z. He, Z. Cheng, H. Yang, D.L. Ma, Nucleic Acids Res. 40 (2012) 941–955.
[40] H.Z. He, K.H. Leung, H. Yang, D.S.H. Chan, C.H. Leung, J. Zhou, A. Bourdoncle, J.L. Mergny, D.L. Ma, Biosens. Bioelectron. 41 (2013) 871–874.
[41] A.E. Friedman, J.C. Chambron, J.P. Sauvage, N.J. Turro, J.K. Barton, J. Am. Chem. Soc. 112 (1990) 4960–4962.
[42] R.M. Hartshorn, J.K. Barton, J. Am. Chem. Soc. 114 (1992) 5919–5925.
[43] C.J. Murphy, J.K. Barton, Methods Enzymol. 226 (1993) 576–594.
[44] Y. Jenkins, A.E. Friedman, N.J. Turro, J.K. Barton, Biochemistry 31 (1992) 10809–10816.
[45] C. Turro, S.H. Bossmann, Y. Jenkins, J.K. Barton, N.J. Turro, J. Am. Chem. Soc. 117 (1995) 9026–9032.
[46] C.G. Coates, J.J. McGarvey, P.L. Callaghan, M. Coletti, J.G. Hamilton, J. Phys. Chem. B 105 (2001) 730–735.
[47] S. Shi, J. Zhao, X. Geng, T. Yao, H. Huang, T. Liu, L. Zheng, Z. Li, D. Yang, L. Ji, Dalton Trans. 39 (2010) 2490–2493.
[48] S. Shi, X. Geng, J. Zhao, T. Yao, C. Wang, D. Yang, L. Zheng, L. Ji, Biochimie 92 (2010) 370–376.
[49] S.A. Tysoe, R. Kopelman, D. Schelzig, Inorg. Chem. 38 (1999) 5196–5197.
[50] J. Bolger, A. Gourdon, E. Ishow, J.P. Launay, Inorg. Chem. 35 (1996) 2937–2944.
[51] Y. Liu, A. Chouai, N.N. Degtyareva, D.A. Lutterman, K.R. Dunbar, C. Turro, J. Am. Chem. Soc. 127 (2005) 10796–10797.
[52] D.A. Lutterman, A. Chouai, Y. Liu, Y.J. Sun, C.D. Stewart, K.R. Dunbar, C. Turro, J. Am. Chem. Soc. 130 (2008) 1163–1170.
[53] S. Shi, J. Zhao, X. Gao, C. Lv, L. Yang, J. Hao, H. Huang, J. Yao, W. Sun, T. Yao, L. Ji, Dalton Trans. 41 (2012) 5789–5793.
[54] J. Yao, X. Gao, W. Sun, X. Fan, S. Shi, T. Yao, Inorg. Chem. 51 (2012) 12591–12593.
[55] C.A. Puckett, R.J. Ernst, J.K. Barton, Dalton Trans. 39 (2010) 1159–1170.
[56] A.C. Komor, J.K. Barton, Chem. Commun. 49 (2013) 3617–3630.
[57] N.P. Cook, V. Torres, D. Jain, A.A. Mart, J. Am. Chem. Soc. 133 (2011) 11121–11123.
[58] W. Sun, T. Yao, S. Shi, Analyst 137 (2012) 1550–1552.
[59] W. Sun, J. Yao, T. Yao, S. Shi, Analyst 138 (2013) 421–424.
[60] W. Sun, S. Shi, T. Yao, Anal. Methods 3 (2011) 2472–2474.
[61] T. Cheng, J. Yao, X. Gao, S. Shi, T. Yao, Analyst 138 (2013) 3483–3489.
[62] K. Xu, J. Huang, Z. Ye, Y. Ying, Y. Li, Sensors 9 (2009) 5534–5557.
[63] K. Healy, Nano Med. 2 (2007) 459–481.
[64] J.J. Li, J.J. Zhu, Analyst 138 (2013) 2506–2515.
[65] H. Wang, R.H. Yang, L. Yang, W.H. Tan, ACS Nano 3 (2009) 2451–2460.
[66] J. Liu, J. Liu, L. Yang, X. Chen, M. Zhang, F. Meng, T. Luo, M. Li, Sensors 9 (2009) 7343–7364.
[67] P. Wu, X.P. Yan, Chem. Soc. Rev. 42 (2013) 5489–5521.
[68] M. Geszke-Moritz, M. Moritz, Mater. Sci. Eng. C 33 (2013) 1008–1021.
[69] D. Zhou, Biochem. Soc. Trans. 40 (2012) 635–639.
[70] Y. Zhang, T.H. Wang, Theranostics 2 (2012) 631–654.
[71] W.R. Algar, K. Susumu, J.B. Delehanty, I.L. Medintz, Anal. Chem. 83 (2011) 8826–8837.
[72] X. Xu, X. Liu, Z. Nie, Y. Pan, M. Guo, S. Yao, Anal. Chem. 83 (2010) 52–59.
[73] R. Freeman, X. Liu, I. Willner, J. Am. Chem. Soc. 133 (2011) 11597–11604.
[74] M. Sykora, M.A. Petruska, J. Alstrum-Acevedo, I. Bezel, T.J. Meyer, V.I. Klimov, J. Am. Chem. Soc. 128 (2006) 9984–9985.
[75] M.G. Sandros, D. Gao, D.E. Benson, J. Am. Chem. Soc. 127 (2005) 12198–12199.
[76] J. Huang, D. Stockwell, Z.Q. Huang, D.L. Mohler, T.Q. Lian, J. Am. Chem. Soc. 130 (2008) 5632–5633.
[77] D. Zhao, W.H. Chan, Z. He, T. Qiu, Anal. Chem. 81 (2009) 3537–3543.
[78] A. Ono, H. Torigoe, Y. Tanakac, I. Okamoto, Chem. Soc. Rev. 40 (2011) 5855–5866.
[79] D. Du, Y. Yang, Y. Lin, MRS Bull. 37 (2012) 1290–1296.
[80] E. Morales-Narváez, A. Merkoçi, Adv. Mater. 24 (2012) 3298–3308.
[81] S. Kochmann, T. Hirsch, O.S. Wolfbeis, Trends Anal. Chem. 39 (2012) 87–113.
[82] W. Putzbach, N.J. Ronkainen, Sensors 13 (2013) 4811–4840.
[83] J. Balapanuru, J.X. Yang, S. Xiao, Q. Bao, M. Jahan, L. Polavarapu, J. Wei, Q.H. Xu, K.P. Loh, Angew. Chem. Int. Ed. 49 (2010) 6549–6553.
[84] H. Dong, W. Gao, F. Yan, H. Ji, H. Ju, Anal. Chem. 82 (2010) 5511–5517.

[85] L. Sheng, J. Ren, Y. Miao, J. Wang, E. Wang, Biosens. Bioelectron. 26 (2011) 3494–3499.
[86] W. Wu, H. Hu, F. Li, L. Wang, J. Gao, J. Lu, C. Fan, Chem. Commun. 47 (2011) 1201–1203.
[87] J.Z. Wu, B.H. Ye, L. Wang, L.N. Ji, J.Y. Zhou, R.H. Li, Z.Y. Zhou, Dalton Trans. 8 (1997) 1395–1402.
[88] E. Amouyal, A. Homsi, J.C. Chambron, J.P. Sauvage, Dalton Trans. 6 (1990) 1841–1845.
[89] H. Peng, L. Zhang, T.H.M. Kjällman, C. Soeller, J. Travas-Sejdic, J. Am. Chem. Soc. 129 (2007) 3048–3049.
[90] W.S. Hummers, R.E. Offeman, J. Am. Chem. Soc. 80 (1958). 1339–1339.
[91] Y. Xu, H. Bai, G. Lu, C. Li, G. Shi, J. Am. Chem. Soc. 130 (2008) 5856–5857.
[92] B.M. Zeglis, V.C. Pierre, J.K. Barton, Chem. Commun. 44 (2007) 4565–4579.
[93] K.E. Erkkila, D.T. Odom, J.K. Barton, Chem. Rev. 99 (1999) 2777–2796.
[94] D.S. Xiang, G.H. Zhou, M. Luo, X.H. Ji, Z.K. He, Analyst 137 (2012) 3787–3793.
[95] L. Zhang, Y. Zhang, M. Wei, Y. Yi, H. Li, S. Yao, New J. Chem. 37 (2013) 1252–1257.
[96] H.Z. He, D.S.H. Chan, C.H. Leung, D.L. Ma, Nucleic Acids Res. 41 (2013) 4345–4359.